

Velocity scaling of granular flow in silos under different discharge modes

Tongtong Mu(牟彤彤), Quan Chen(陈泉), Wenjing Wang(王文静), Ran Li(李然), Ge Sun(孙歌), and Hui Yang(杨晖)

Citation: Chin. Phys. B, 2026, 35 (**4**): 044701. DOI: 10.1088/1674-1056/ae12d7
http://cpb.iphy.ac.cn; http://iopscience.iop.org/cpb

What follows is a list of articles you may be interested in

Molecular dynamics simulation of the flow mechanism of shear-thinning fluids in a microchannel

Gang Yang(杨刚), Ting Zheng(郑庭), Qihao Cheng(程启昊), and Huichen Zhang(张会臣)
Chin. Phys. B, 2024, 33 (**4**): 044701. DOI: 10.1088/1674-1056/ad08a7

Effect of particle shape on packing fraction and velocity profiles at outlet of a silo

Qing-Qing Gao(高庆庆), Yu-Chao Chen(陈玉超), and Lin Hu(胡林)
Chin. Phys. B, 2023, 32 (**6**): 064702. DOI: 10.1088/1674-1056/aca204

Discharge and flow characterizations of the double-side sliding discharge plasma actuator

Qi-Kun He(贺启坤), Hua Liang(梁华), Bo-Rui Zheng(郑博睿)
Chin. Phys. B, 2020, 29 (**6**): 064702. DOI: 10.1088/1674-1056/ab8624

Dynamic evolution of vortex structures induced bytri-electrode plasma actuator

Bo-Rui Zheng(郑博睿), Ming Xue(薛明), Chang Ge(葛畅)
Chin. Phys. B, 2020, 29 (**2**): 024704. DOI: 10.1088/1674-1056/ab671f

Active control of wall-bounded turbulence for drag reduction with piezoelectric oscillators

Jian-Xia Bai(白建侠), Nan Jiang(姜楠), Xiao-Bo Zheng(郑小波), Zhan-Qi Tang(唐湛琪), Kang-Jun Wang(王康俊), Xiao-Tong Cui(崔晓通)
Chin. Phys. B, 2018, 27 (**7**): 074701. DOI: 10.1088/1674-1056/27/7/074701

Velocity scaling of granular flow in silos under different discharge modes

Tongtong Mu(牟彤彤)[1,2], Quan Chen(陈泉)[1], Wenjing Wang(王文静)[3], Ran Li(李然)[1], Ge Sun(孙歌)[1,2], and Hui Yang(杨晖)[2,1,†]

[1] *School of Optical-Electrical and Computer Engineering, University of Shanghai for Science and Technology, Shanghai* 200093, *China*
[2] *College of Medical Instrumentation, Shanghai University of Medicine and Health Sciences, Shanghai* 201318, *China*
[3] *School of Physical Science and Technology, ShanghaiTech University, Shanghai* 201318, *China*

(Received 19 August 2025; revised manuscript received 8 October 2025; accepted manuscript online 14 October 2025)

Accurately measuring the velocity field of granular flow in silos and elucidating the distribution law under different discharge modes are essential for understanding the mechanisms of granular rheology and optimizing discharge system design. This work investigates the flow characteristics of black electroplated glass beads in a two-dimensional silo under free-fall discharge and conveyor-belt discharge. The particle tracking velocimetry (PTV) method is employed to measure the velocity field, and the distribution characteristics under the two modes are systematically compared and analyzed. The results show that although there are significant differences in the numerical values of granular velocity, the normalized velocity profiles remain highly consistent. On this basis, a quantitative relationship between the velocity profiles under the two discharge modes is established through the kinematic model. This reveals that the differences in velocity profiles caused by the discharge modes essentially correspond to magnitude scaling, while the overall flow characteristics remain invariant. This finding not only provides a predictive model for the velocity field under conveyor-belt discharge in silos but also contributes empirical data to advance the rheological theory of granular flow.

Keywords: velocity profile, granular flow, silo, discharge

PACS: 47.57.Gc, 47.57.–s, 47.80.Cb

DOI: 10.1088/1674-1056/ae12d7 **CSTR:** 32038.14.CPB.ae12d7

1. Introduction

Free fall discharge and conveyor belt discharge are two primary modes for silo emptying.[1–3] Among them, free fall discharge has been widely studied due to its cost-free transport, and the velocity profiles of granular flow can be described by the kinematic model.[4,5] However, its mass discharge rate (MDR) is constrained by orifice size and granular properties, and therefore cannot meet the demand for variable MDR in industrial and agricultural applications. The installation of a conveyor belt below a silo effectively resolves this limitation, with precise control of MDR achieved by regulating the belt velocity.[6,7] Since the conveyor belt can alter the motion state of discrete particles, there is currently no model that describes the velocity profiles under this mode. Notably, while MDR differs between discharge modes, other conditions remain identical, such as silo geometry, particle size, and frictional coefficients. Therefore, accurately measuring the velocity profiles and correlating the flow characteristics of the two discharge modes are key steps in developing a predictive model for conveyor belt discharge, which is crucial for the precise control of silo discharge.

For the velocity profiles of granular flow under free fall discharge in silos, researchers have carried out numerous studies. Based on the random movement of discrete particles, Nedderman and Tüzün first proposed a kinematic model to describe the velocity field in silos. This model did not involve stress–strain coupling and simplified the complex interactions between particles, but its parameters lacked clear physical definitions.[8,9] Hsiau and Hunt[10] and Natarajan *et al.*[11] studied the flow behavior of glass beads during silo discharge through an imaging method. They identified the empirical parameters in the kinematic model as the diffusion length, and revealed that this parameter differs between the transverse and flow directions. Chen *et al.*[12] used the PTV method to measure the velocity profiles during steady-state flow in a flat-bottomed silo, and established a relationship between diffusion length and granular temperature based on the kinematic model. This result revealed the connection between the kinematic model and the microscopic motion of particles. In addition, Medina *et al.*[13] and Zuriguel *et al.*[14] validated that the kinematic model can accurately describe the velocity fields in two-dimensional (2D) and three-dimensional (3D) silos during free fall discharge, however, its applicability is limited to the converging zone. Conveyor belt discharge is a widely adopted mode for granular material transport in industrial and agricultural silos, and has attracted attention because it decouples the granular velocity from the orifice size.[15] Gella *et al.*[16] measured the velocity fields during 2D silo discharge with differ-

†Corresponding author. E-mail: yangh_23@sumhs.edu.cn

© 2026 Chinese Physical Society and IOP Publishing Ltd. All rights, including for text and data mining, AI training, and similar technologies, are reserved.

ent orifice sizes and conveyor belt velocities. They found that the velocity profiles for a fixed orifice could collapse into a single curve under varying belt velocities. This scaling behavior aligns with the self-similar velocity profile reported by Janda *et al.*[17] under free fall discharge. Surprisingly, Gella *et al.*[18] and Fan *et al.*[19] discovered that the vertical velocity decreases with increasing orifice size at the same belt velocity in a study of the flow characteristics of ellipsoidal particles in conveyor-controlled silos. This trend opposes the velocity–orifice relationship under free fall discharge, where granular velocities increase with orifice enlargement. The aforementioned studies demonstrate both connections and distinctions in the velocity profiles of granular flow under the two discharge modes, and even show inverse trends. Therefore, accurate measurement of the velocity fields and systematic comparison of the similarities and differences in velocity profiles under both discharge modes are key steps toward establishing a velocity profile model for conveyor belt discharge in silos.

This study utilizes the PTV method to measure the velocity fields of glass beads in a 2D flat-bottom silo under free fall and conveyor belt discharge modes. By comparing both velocity magnitudes and normalized profiles, the differences and consistencies in flow characteristics induced by the discharge modes are revealed. Based on this result, the kinematic model originally developed for free fall discharge is applied to fit the velocity profiles under conveyor belt discharge. Ultimately, a quantitative relationship model capable of accurately describing the velocity profiles under both discharge modes is established.

2. Experimental setup and method

2.1. Experimental system

Figure 1(a) shows the experimental system diagram, which consists of a 2D flat-bottom rectangular silo, a camera, an LED light, an electronic scale, and a conveyor belt. The silo has an available space of 500×150 mm^2, and its front and rear walls are made of 10 mm-thick transparent plexiglass plates spaced 8 mm apart. The bottom of the silo is enclosed with a 2.5 mm-thick plexiglass plate with a rectangular orifice. To prevent jamming events, the orifice size D is selected as 20 mm. The filling material consists of black electroplated glass beads with a diameter range of $d_\mathrm{p} \in [2, 2.5]$ mm and a density of $\rho_\mathrm{p} = 2490$ kg/m^3. The camera (Revealer, M230-16G) is used to capture granular motion during the discharge process, with a frame rate set to 200 fps. The LED light (Godox, SL200W III) provides illumination for the camera. The electronic scale (Lucky, CN-LGC30001) records the MDR of granular flow during discharge with an accuracy of 0.1 g. The coordinate system is established with the center of the orifice at the silo bottom as the origin. For the conveyor belt discharge experiments, a velocity-adjustable conveyor belt is placed directly below the silo orifice. To effectively control the MDR of particles in the silo, the distance h_d between the silo bottom and the belt is set to $2d_\mathrm{p}$, as shown in Fig. 1(b). The adjustment of the conveyor belt velocity v_b is achieved by varying the motor speed w_n, and their corresponding relationship is shown in Fig. 1(c). Specifically, the conveyor belt velocity presents a linear dependence on the motor speed, and can be adjusted within the range of 14.1 mm/s to 286.9 mm/s at $w_\mathrm{n} \in [150, 3000]$ rpm. When the motor speed w_n is less than 150 rpm, the conveyor belt remains stationary due to frictional resistance. In this study, silo discharge experiments are conducted under two modes: free fall discharge (FFD) and conveyor belt discharge (CBD). For the CBD, three conveyor belt velocities of low, medium, and high are selected, corresponding to 95.4 mm/s, 191.2 mm/s, and 286.9 mm/s (denoted as CBD1, CBD2, and CBD3), respectively.

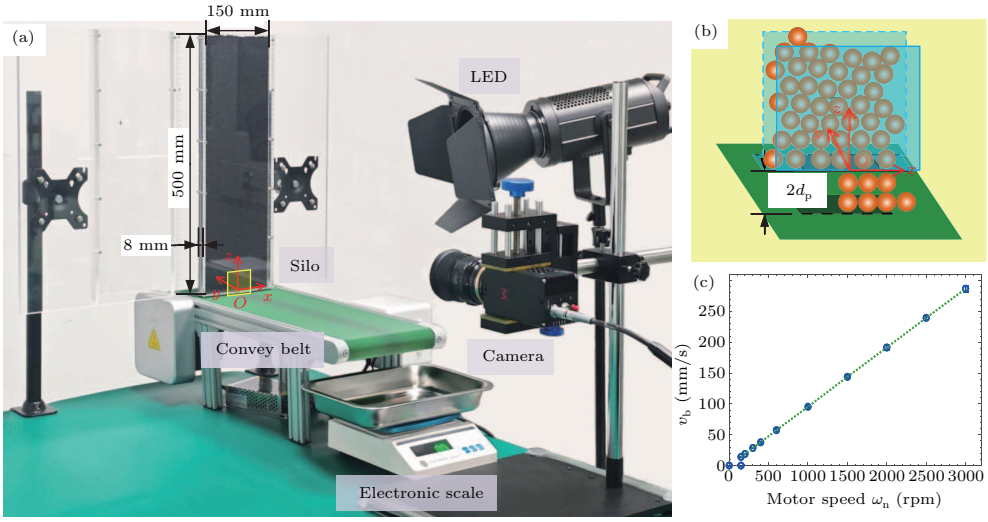


Fig. 1. (a) Experimental setup; (b) annotated photograph of the distance between the silo bottom and the belt; (c) response of the conveyor belt to the motor speed.

2.2. Measurement method

Due to the challenges of high particle density, large velocity gradients, and a non-uniform flow field during silo discharge, the PTV method based on the pyramidal Lucas–Kanade (LK) optical flow algorithm[20] is utilized in this work to calculate the velocity field of granular flow, and its principle is shown in Fig. 2. This method requires three conditions, namely brightness constancy, small motion, and spatial consistency. Figure 2(a) shows two adjacent frames. Firstly, the Shi–Tomasi algorithm[21] is used to detect corners in the images, as illustrated in Fig. 2(b). Subsequently, the pyramidal LK optical flow algorithm[22] is applied to track these corners and obtain their displacements, with the results presented in Fig. 2(c). The detailed process is as follows: the image pyramid with different resolutions is initially constructed. Based on the minimum residual between images, the optical flow estimation is performed using the iterative LK algorithm starting from the highest layer of the pyramid. The results are then passed to the next layer as the initial value and transferred gradually until the lowest layer. Ultimately, the optical flow vectors in the original image represent the displacements (Δx, Δz) of the corners. Figure 2(d) shows the vector velocity field. The vector velocity of particles, $\boldsymbol{u}_i = (u_{xi}, u_{zi})$, is calculated as the ratio of the displacement to the time interval Δt between two adjacent frames

$$\begin{cases} u_{xi} = \Delta x_i / \Delta t, \\ u_{zi} = \Delta z_i / \Delta t. \end{cases} \tag{1}$$

Here, u_x and u_z are the components of the instantaneous velocity vector $\boldsymbol{u}$ of particle i along the x- and z-directions, respectively. This method effectively enhances the tracking accuracy of complex granular flow fields. Even at the orifice with a relatively high flow rate, the error remains within 1%.[20] To ensure the precise capture of the details of granular flow, the silo is discretized into multiple boxes of size $1.5d_\mathrm{p} \times 1.5d_\mathrm{p}$.[23] All the instantaneous velocities passing through each box within a time period are calculated to construct the average velocity field. The component expression of the average velocity within each box is

$$\begin{cases} v_x = \dfrac{1}{N_\mathrm{b}} \sum\limits_{i=1}^{N_\mathrm{b}} u_{xi}, \\ v_z = \dfrac{1}{N_\mathrm{b}} \sum\limits_{i=1}^{N_\mathrm{b}} u_{zi}, \end{cases} \tag{2}$$

where v_x and v_z are the x and z components of the mean velocity vector $\boldsymbol{v}$ in the box, respectively, and N_b is the number of particles flowing through the box. The magnitude of the mean velocity is given by $v(x,z) = (v_x^2 + v_z^2)^{1/2}$.

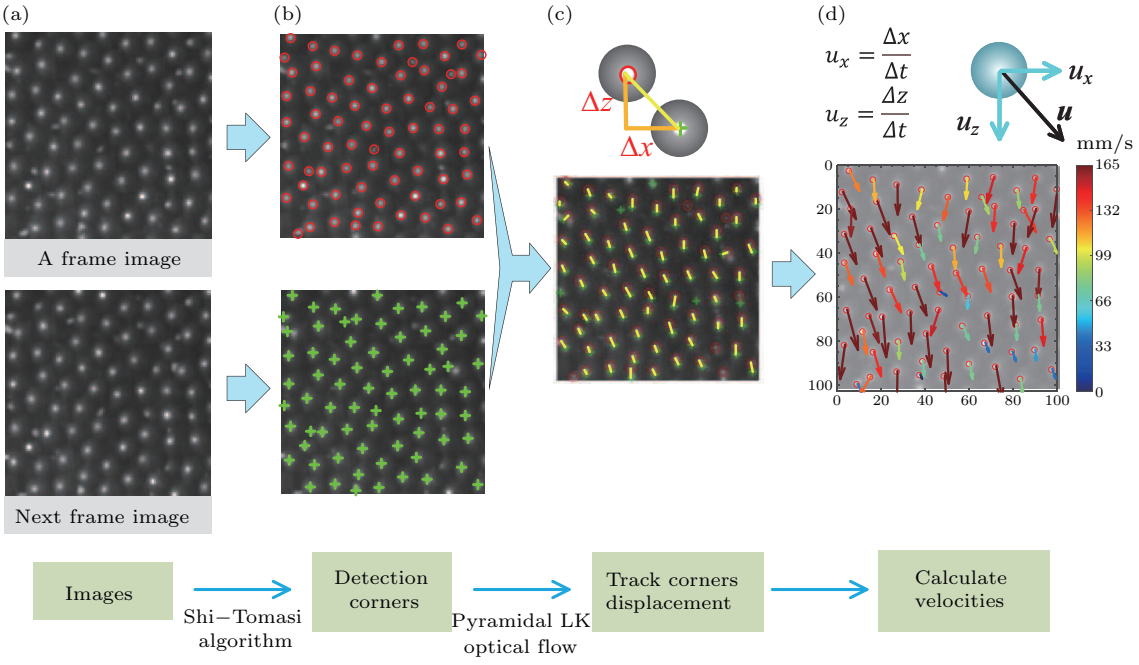


Fig. 2. Schematic diagram of the PTV method based on the pyramidal Lucas–Kanade (LK) optical flow algorithm.

3. Results and discussion

3.1. Distribution characteristics of the velocity field

3.1.1. Difference

Figure 3 illustrates the velocity field of granular flow in silos under free fall and conveyor belt discharge. Figure 3(a) shows the velocity contours (solid lines) and the stagnant zone boundary (dotted line), which is defined as the location where the velocity drops to 1% of the central velocity v_c at each height. Figures 3(b) and 3(c) present the vertical and horizontal velocity profiles, respectively. It can be seen that the

spatial distributions of the velocity field under the two discharge modes are similar. The maximum velocity occurs at the orifice and decreases upward along the z-axis, with consistent trends observed in the vertical and horizontal velocity components. However, differences exist in the velocity magnitude and in the extent of the stagnant zone. The contours under free fall discharge are denser, indicating higher velocities than those under conveyor belt discharge, as further confirmed in Figs. 3(b) and 3(c). These results indicate that the conveyor belt reduces the overall granular velocity, resulting in a more uniform velocity field, which is consistent with the results reported by Fan *et al.*[19] Moreover, the height of the stagnant zone is significantly greater under conveyor belt discharge than under free fall discharge and remains independent of the belt velocity. This phenomenon, observed for the first time, can be explained by the conveyor belt restricting particle outflow at the orifice, which results in particle accumulation and an upward expansion of the stagnant zone.

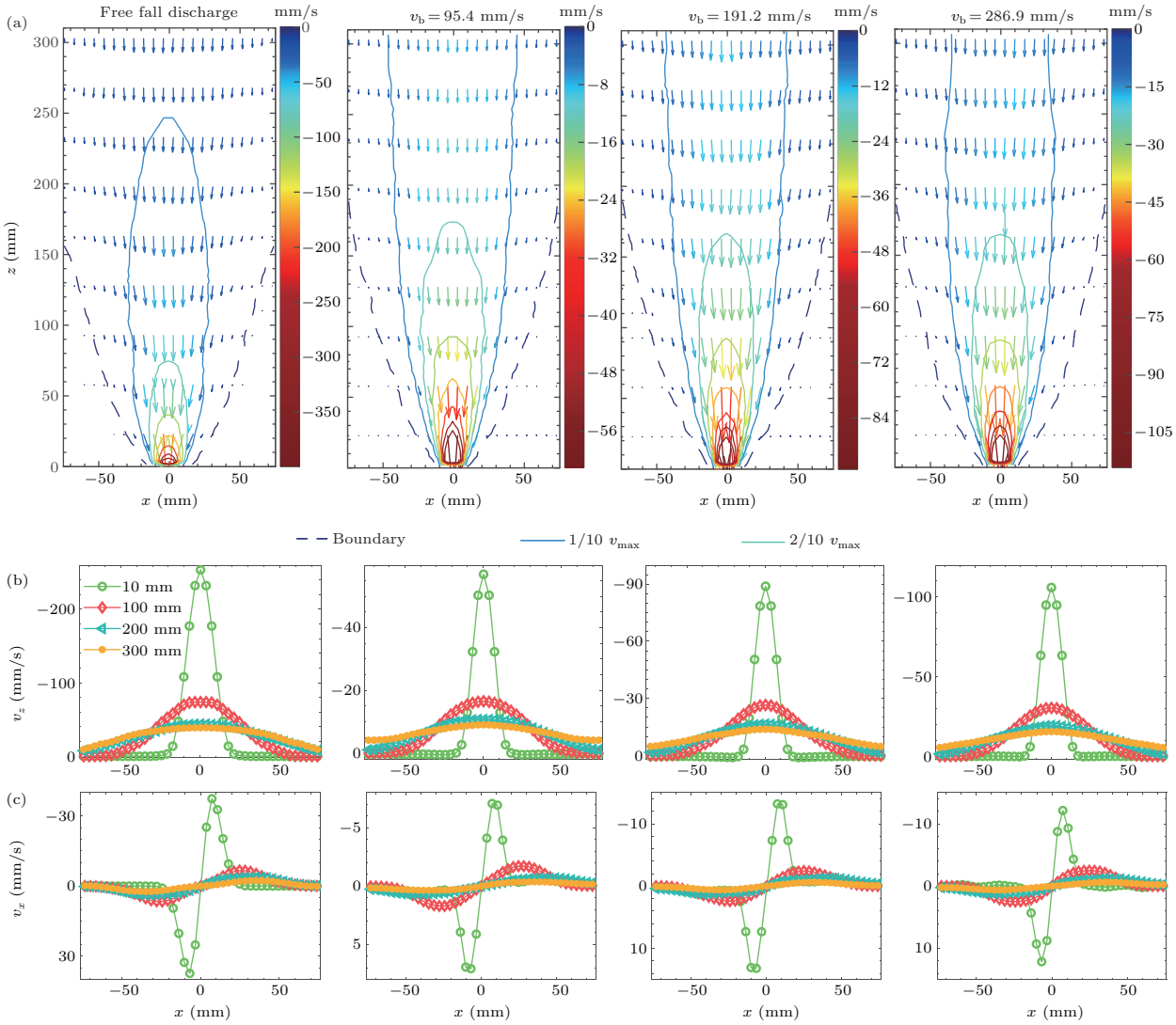


Fig. 3. Velocity fields of granular flow in silos. From left to right: FFD, CBD1, CBD2, and CBD3. (a) Velocity field contours (solid lines) and stagnant zone boundary (dotted line); (b) vertical velocity profiles v_z; (c) horizontal velocity profiles v_x.

Figure 4 shows the maximum velocities in the vertical and horizontal directions at different silo heights under free fall and conveyor belt discharge. Table 1 lists the maximum velocities and velocity ratios for the two discharge modes. It can be seen that the variation trends of granular velocities at different heights are similar. Taking $z = 10$ mm as an example, the maximum vertical velocities are 55.8 mm/s, 85.2 mm/s, and 103.0 mm/s under conveyor belt discharge, respectively, which are only 22.0%, 33.6%, and 40.6% of the values under free fall discharge. More significantly, the horizontal velocities are only 15.2%, 29.7%, and 33.4% of those under free fall discharge. These results demonstrate that conveyor belt discharge significantly reduces the granular velocity in silos. Moreover, the maximum velocity exhibits an increasing trend with increasing belt velocity, although its growth rate gradually decreases. On the other hand, the maximum velocity gradually decreases as the height increases, whereas the velocity ratio between the two discharge modes shows an opposite trend.

This indicates that the regulating effect of the conveyor belt on granular motion gradually weakens with increasing height. This phenomenon can be attributed to spatial variations in the kinematic behavior of the particles.[24] Near the silo base, the granular velocity is jointly regulated by gravitational acceleration and conveyor belt movement, and thus shows a strong correlation with the belt velocity. In the upper region, however, particle–wall and particle–particle frictional interactions become the dominant dissipative mechanisms, which diminish the influence of the conveyor belt.

Table 1. The maximum values of velocity and the ratios of two discharge modes in vertical and horizontal directions at different heights.

z (mm)	Discharge modes	$\|v_z\|_{\max}$ (mm/s)	$\|v_x\|_{\max}$ (mm/s)	Ratio of $\|v_z\|_{\max}$	Ratio of $\|v_x\|_{\max}$
10	FFD	253.6	37.4	–	–
	CBD1	55.8	5.7	22.0%	15.2%
	CBD2	85.2	11.1	33.6%	29.7%
	CBD3	103.0	12.5	40.6%	33.4%
100	FFD	73.7	7.3	–	–
	CBD1	18.3	2.3	24.8%	31.5%
	CBD2	26.4	2.8	35.8%	38.4%
	CBD3	30.2	3.2	41.0%	43.8%
200	FFD	43.4	4.2	–	–
	CBD1	11.3	0.7	26.0%	16.7%
	CBD2	15.9	1.3	36.6%	31.0%
	CBD3	18.3	1.5	42.2%	35.7%
300	FFD	39.0	2.3	–	–
	CBD1	8.8	0.5	22.6%	21.7%
	CBD2	12.9	0.9	33.1%	39.1%
	CBD3	15.8	1.1	40.5%	47.8%

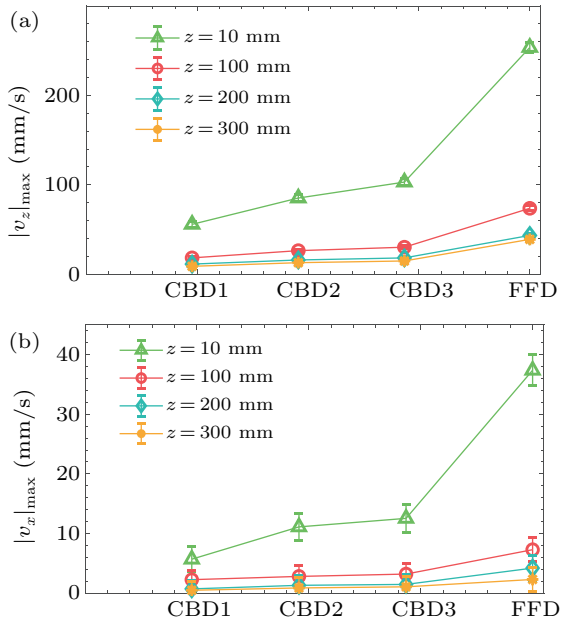


Fig. 4. Maximum velocities at different silo heights under FFD and CBD in the vertical direction (a) and horizontal direction (b).

3.1.2. Consistency

In the previous section, the similarity of the velocity distributions under different discharge modes was observed. To further validate this result, the vertical and horizontal velocities are normalized by their respective maximum velocities at various heights ($z = 10$ mm, 100 mm, 200 mm, 300 mm), i.e., $\bar{v}_z = v_z/|v_z|_{\max}$ and $\bar{v}_x = v_x/|v_x|_{\max}$. The normalized velocity profiles are shown in Fig. 5. It can be observed that they collapse into a single curve, especially for $z < 200$ mm. This is consistent with the self-similarity in orifice velocity profiles reported by Gella *et al.*,[16] and indicates that the spatial distributions of velocity are independent of the discharge mode and belt velocity. This behavior occurs because the flow dynamics are primarily dominated by the silo geometry (such as wall friction, geometric configuration, and orifice size) and granular properties (such as particle shape, density, and internal friction), which define flow boundaries and interparticle interactions, respectively.[25–27] Thus, conveyor belt discharge only modulates the velocity magnitude of granular motion.

To quantify the similarity between velocity profiles under different discharge modes, a Pearson correlation analysis is performed on the normalized velocities. The correlation coefficients are presented in Table 2, where ρ_z and ρ_x correspond to the vertical and horizontal velocity components, respectively. It is found that the correlation coefficients for both vertical and horizontal velocity profiles exceed 0.91, with values approaching 1 in the region where $z < 200$ mm. This strong linear correlation indicates that the velocity profiles under free fall and conveyor belt discharge are essentially identical in shape, differing only in magnitude. These findings confirm that conveyor belt discharge merely scales the velocity magnitude without altering the spatial distribution, as it imposes a controlled boundary condition only at the orifice. This result can be attributed to the fact that the dominant driving force for granular flow in both discharge modes is gravity, which

acts uniformly across the entire flow field.[28] Consequently, granular flow in silos exhibits self-similar characteristics, independent of the discharge mode.[17]

Based on the differences and consistencies of the velocity profiles under the two discharge modes, it can be inferred that the kinematic model for the velocity profile under free fall discharge can also be applied to describe the profile under conveyor belt discharge.

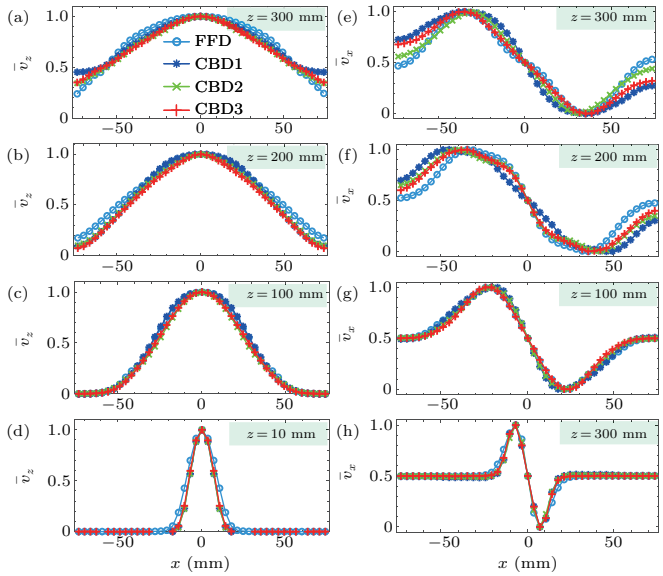


Fig. 5. Normalized velocity profiles of granular flow at different heights. (a)–(d) normalized vertical velocities; (e)–(h) normalized horizontal velocities.

Table 2. Correlation coefficients of normalized velocity profile under different discharge modes.

z (mm)		ρ_z	ρ_x
300	FFD vs CBD1	0.97	0.94
	FFD vs CBD2	0.98	0.97
	FFD vs CBD3	0.98	0.96
200	FFD vs CBD1	1.00	0.91
	FFD vs CBD2	1.00	0.96
	FFD vs CBD3	1.00	0.98
100	FFD vs CBD1	1.00	1.00
	FFD vs CBD2	1.00	1.00
	FFD vs CBD3	1.00	0.99
10	FFD vs CBD1	0.98	0.98
	FFD vs CBD2	0.98	0.99
	FFD vs CBD3	0.99	0.99

3.2. Kinematic model of the velocity profile

The kinematic model proposed by Nedderman and Tüzün describes the velocity field of particles during the silo discharge process, and its governing equations are

$$\begin{cases} v_z = a_z \exp\left(-\dfrac{x^2}{4b_z z}\right), \\ v_x = -b_x \dfrac{\partial v_z}{\partial x}, \end{cases} \tag{3}$$

where the fitting parameter a_z represents the central velocity v_c in the silo, and b_z denotes the diffusion length associated with the random movement of particles. Since the horizontal velocity v_x depends on the gradient of the vertical velocity v_z along the x-direction, only the vertical velocity v_z will be fitted and analyzed in the following.

Figure 6 shows the fitting results of the velocity profile. To quantify the deviation between the measured velocity v_z and the model-predicted velocity $\hat{v}_z$, the normalized root mean squared error (NRMSE) is adopted as the evaluation metric. This metric normalizes the root mean squared error (RMSE) by the average velocity $\bar{v}_z$ to eliminate dimensional effects, and is defined as

$$\mathrm{NRMSE} = \frac{\mathrm{RMSE}}{\bar{v}_z} = \frac{\sqrt{\frac{1}{N}\sum(v_{zi} - \hat{v}_{zi})^2}}{\bar{v}_z} \times 100\%. \tag{4}$$

The distribution of NRMSE is presented in Fig. 6(a), where a value of 10% serves as the threshold for fitting validity.[29] The results demonstrate that under free fall discharge, the error remains below 10% within the converging zone ($z \leq 159$ mm). Beyond this region, the error progressively increases to 20%, indicating significant deviation between the measured velocity profiles and model predictions. Remarkably, under conveyor belt discharge, NRMSE consistently remains below 10% throughout the silo height, confirming that the kinematic model accurately describes the velocity profiles of discrete particles.

Figure 6(b) illustrates the correlation between the parameter a_z and the granular velocity v_c at the silo center. It shows that, in both free fall and conveyor belt discharge, a_z remains approximately equal to v_c, consistent with the results of Medina *et al.*[13] for free fall discharge. Figure 6(c) characterizes the distribution of the diffusion length b_z, which increases with silo height for both discharge modes. Notably, b_z is nearly identical across different belt velocities. Compared with free fall discharge, the deviation of b_z is relatively small, with RMSEs of 0.55 mm, 0.47 mm, and 0.52 mm, all less than one particle diameter. This indicates that conveyor belt discharge does not achieve complete decoupling between granular motion and silo geometry. It should be emphasized that the parameters a_z and b_z beyond the converging zone in free fall discharge (Figs. 6(b) and 6(c)) lack statistical validity due to excessive fitting error.

In conclusion, the differences in the velocity profile caused by varying belt velocities manifest primarily in the parameter a_z, while exerting negligible influence on the diffusion length b_z. Consequently, the key to developing a velocity profile model for conveyor belt discharge lies in establishing the relationship between the parameter a_z and the belt velocity v_b.

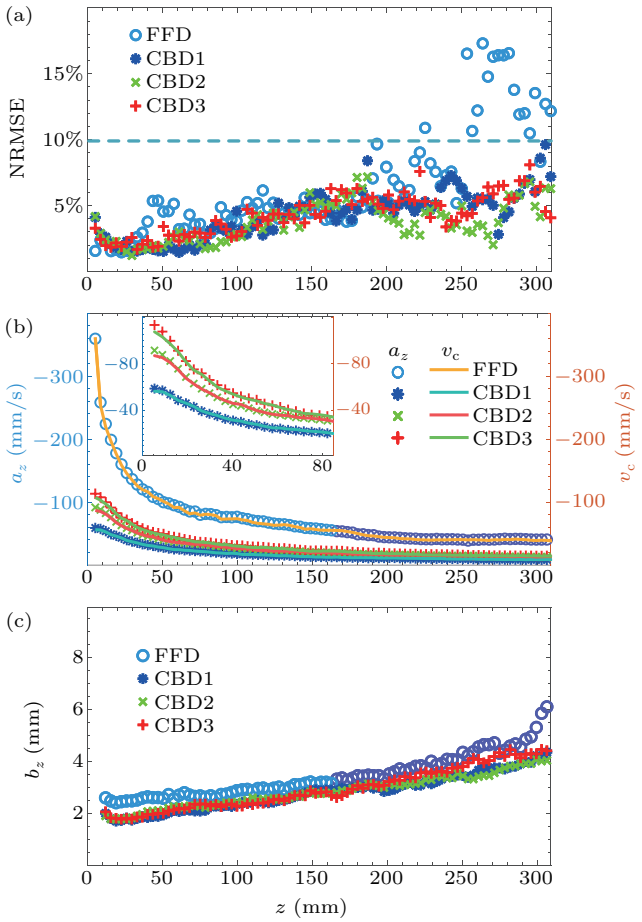


Fig. 6. Fitting results of the kinematic model for the vertical velocity profile at different heights. (a) NRMSE; (b) relationship between parameter a_z and the central velocity v_c at the silo center; (c) distribution of the diffusion length b_z.

To establish the relationship between velocity profiles under free fall discharge and conveyor belt discharge (denoted as $v_{z,\mathrm{F}}$ and $v_{z,\mathrm{B}}$), the velocity ratio is analyzed

$$\frac{v_{z,\mathrm{B}}}{v_{z,\mathrm{F}}} = \frac{a_{z,\mathrm{B}} \exp\left(-\frac{x^2}{4b_{z,\mathrm{B}}z}\right)}{a_{z,\mathrm{F}} \exp\left(-\frac{x^2}{4b_{z,\mathrm{F}}z}\right)}, \tag{5}$$

where $a_{z,\mathrm{B}}$, $b_{z,\mathrm{B}}$ and $a_{z,\mathrm{F}}$, $b_{z,\mathrm{F}}$ are the parameters of the velocity profile models. Given the near-equality of the diffusion lengths for the two discharge modes, the ratio of the exponential terms approaches unity. Thus, Eq. (5) can be simplified to the ratio of the parameter a_z

$$\frac{v_{z,\mathrm{B}}}{v_{z,\mathrm{F}}} \approx \frac{a_{z,\mathrm{B}}}{a_{z,\mathrm{F}}}. \tag{6}$$

Further, define the parameter k as

$$k \equiv \frac{a_{z,\mathrm{B}}}{a_{z,\mathrm{F}}} = \frac{v_{c,\mathrm{B}}}{v_{c,\mathrm{F}}}. \tag{7}$$

Figure 7(a) depicts the variation of parameter k with silo height under different belt velocities. To accurately investigate the variation of k, three additional sets of conveyor belt discharge experiments are conducted at belt velocities v_b of 47.5 mm/s, 143.3 mm/s, and 239.0 mm/s. It is observed that k remains virtually invariant with silo height across all belt velocity conditions, indicating that the belt velocity v_b is the primary determinant of k. Further analysis reveals a positive correlation between k and v_b, as shown in Fig. 7(b). This aligns with the observed increase of the MDR with belt velocity reported by Gella *et al.*,[16] who noted that MDR variations follow a power law. Consequently, a power-law function is employed to fit the relationship between parameter k and belt velocity v_b

$$k = 1 - 0.44 \times v_\mathrm{b}^{-0.22}, \tag{8}$$

where the dimension of v_b is m/s, and the fitting error is 7.4%. Therefore, the vertical velocity distribution $v_{z,\mathrm{B}}$ of particles during conveyor belt discharge is expressed as

$$v_{z,\mathrm{B}} = k v_{z,\mathrm{F}} = \left(1 - 0.44 \times v_\mathrm{b}^{-0.22}\right) a_{z,\mathrm{F}} \exp\left(-\frac{x^2}{4b_{z,\mathrm{F}}z}\right). \tag{9}$$

Equation (9) establishes a quantitative relationship between the velocity profiles of granular flow under the two discharge modes in silos. While this model is derived from statistical analysis of the velocity distribution characteristics, it provides critical guidance for predicting discharge stability across varying belt velocities and for optimizing silo-conveyor system design. Notably, within the tested belt velocity range, the phenomenon of granular velocity eventually approaching that of free fall discharge has not yet been observed. Future work will extend the belt velocity range to further validate the universality of the model.

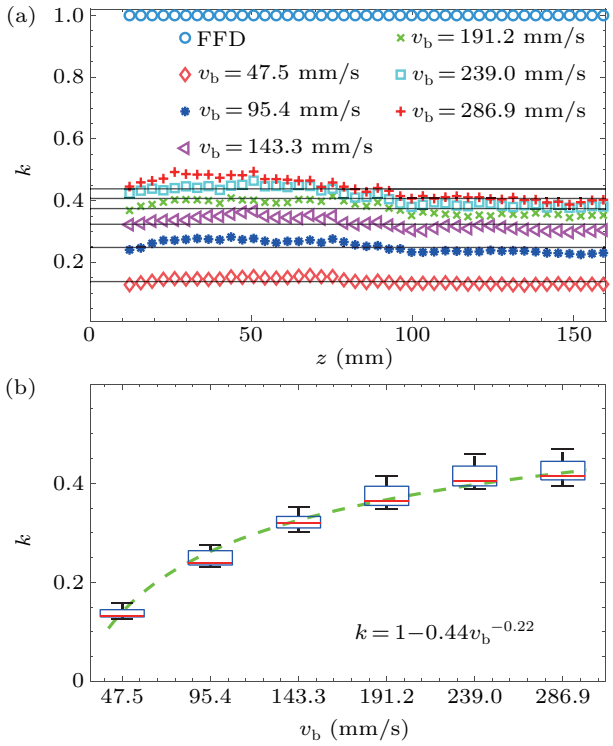


Fig. 7. Variation of parameter k. (a) Variation of k with silo height; (b) variation of k with conveyor belt velocity v_b.

4. Conclusion

In this study, the PTV method was utilized to measure the vector velocity of black electroplated glass beads in a 2D flat-bottomed silo under two distinct modes: free fall discharge and conveyor belt discharge. Systematic analysis of the velocities at different silo heights shows that, despite significant differences in magnitude, the normalized velocity profiles for the two modes exhibit strong overlap. This finding indicates that the velocity profiles of granular flow are self-similar under different discharge modes. Conveyor belt discharge is shown to reduce particle velocities and produce a more uniform velocity field while preserving the intrinsic spatial distribution characteristics. Notably, the height of the stagnant zone remains invariant with variations in belt velocity and is higher than that observed under free fall discharge.

Furthermore, this study confirms that the kinematic model, originally developed for free fall discharge, can be extended to conveyor belt discharge, which has not been previously validated. Crucially, we demonstrate that the model accurately describes the velocity profile across the entire silo height under conveyor belt discharge, whereas in free fall discharge it is valid only within the converging zone. By integrating belt velocity into the model parameters, we establish a quantitative relationship between belt velocity and the velocity profile. This relationship enables a predictive model for granular flow under conveyor-controlled silo discharge, despite being derived from a specific set of experimental conditions. Collectively, these findings deepen the understanding of granular flow under external control and provide a theoretical basis for optimizing the efficient handling of bulk materials in industrial and agricultural silo systems.

Acknowledgments

This work was supported by the National Natural Science Foundation of China (Grant Nos. 12202280 and 12372384) and the Shanghai Municipal Education Commission AI Program (Grant No. SHJWAIJK241201).

References

[1] Mu Y F, Yao T A, Jia H J, Yu X D, Zhao B, Zhang X S, Ni C W and Du L J 2020 *Appl. Energy* **275** 115368
[2] Huang T C, Wu B, Xie F P, Qian H Y, Li Z, Chen P and Xiang Q X 2024 *Biosyst. Eng.* **245** 96
[3] Jiang S Y, Tu J Y, Yang X T and Gui N 2019 *Exp. Comput. Multiph. Flow* **1** 159
[4] Bhateja A 2020 *Phys. Rev. E* **102** 042904
[5] Choi J, Kudrolli A and Bazant M Z 2005 *J. Phys.: Condens. Matter* **17** S2533
[6] Bao D S, Zhang X S, Xu G L, Pan Z Q, Tang X W and Lu K Q 2003 *Phys. Rev. E* **67** 062301
[7] Gella D, Zuriguel I and Maza D 2020 *Phys. Rev. Lett.* **121** 138001
[8] Nedderman R and Tüzün U 1979 *Powder Technol.* **22** 243
[9] Nedderman R, Tüzün U, Savage S and Houlsby G 1982 *Chem. Eng. Sci.* **37** 1597
[10] Hsiau S S and Hunt M L 1993 *J. Fluid Mech.* **251** 299
[11] Natarajan V V R, Hunt M L and Taylor E D 1995 *J. Fluid Mech.* **304** 1
[12] Chen Q, Li R, Xiu W Z, Zivkovic V and Yang H 2021 *Powder Technol.* **392** 123
[13] Medina A, Córdova J, Luna E and Treviño C 1998 *Phys. Lett. A* **250** 111
[14] Zuriguel I, Maza D, Janda A, Hidalgo R C and Garcimartín A 2019 *Granular Matter* **21** 47
[15] Gella D, Zuriguel I and Ortín J 2019 *Phys. Rev. Lett.* **123** 218004
[16] Gella D, Maza D and Zuriguel I 2020 *Powder Technol.* **360** 104
[17] Janda A, Zuriguel I and Maza D 2012 *Phys. Rev. Lett.* **108** 248001
[18] Gella D, Maza D and Zuriguel I 2021 *J. Fluid Mech.* **925** A24
[19] Fan B, Zuriguel I, Dijksman J A, Gucht J and Börzsönyi T 2023 *Phys. Rev. E* **108** 044902
[20] Wang B D, Song J, Li R, Han R, Zheng G and Yang H 2020 *Chin. Phys. B* **29** 014207
[21] Shi J and Tomasi 1994 *Proceedings of IEEE Conference on Computer Vision and Pattern Recognition*, June 21–23, 1994, Seattle, WA, USA, pp. 593
[22] Sharmin N and Brad R 2012 *Sensors* **12** 12694
[23] Sun G, Chen Q, Li R, Zheng Z, Xin Y J and Yang H 2022 *Powder Technol.* **409** 117770
[24] Shi S S, Wu P, Jiang M X, Chen B D, Zhang S P, Dong C Y and Wang L 2025 *Powder Technol.* **452** 120562
[25] Zhu H and Yu A B 2005 *Granular Matter* **7** 97
[26] Cruz F, Emam S, Prochnow M, Roux J N and Chevoir F 2005 *Phys. Rev. E* **72** 021309
[27] Laurent B, Krzysztof G, Selam W, Konrad M, Jerome A and Eric M 2020 *Comput. Electron. Agric.* **172** 105346
[28] Zhu H, Yu A B and Wu Y 2006 *Powder Technol.* **170** 125
[29] Alani O, Abraim M, Ghennioui H, Ghennioui A, Ikenbi I and Dahr F E 2021 *Energy Rep.* **7** 888